This paper was recommended for publication in revised form by Regional Editor Mohammed Sajjad Mayeed

CHARACTERIZATION OF THE EFFECTS OF INSULATING WALL PAINT ON SPACE CONDITIONING IN A ROOM

David J. Buckmaster
Department of Mechanical Engineering
Case Western Reserve University
10900 Euclid Ave, Cleveland, OH, USA

***Alexis R. Abramson**
Department of Mechanical Engineering
Case Western Reserve University
10900 Euclid Ave, Cleveland, OH, USA

ABSTRACT

Manufacturers of "insulating paints" continue to enter the marketplace with claims of their products' exceptional potential to reduce building energy consumption. To help dispel this myth, this paper presents the simple theoretical analysis disproving this claim, backed by a more in-depth computational fluid dynamics (CFD) analysis testing the performance of such products. The CFD analysis is conducted in a simulation of a room as a function of various parameters. The benefits of insulating paint are shown to be minimal; even under highly favorable conditions, energy consumption is reduced by less than 1%.

INTRODUCTION

Energy use in residential and commercial buildings accounts for up to 40% of primary energy consumption depending on climate region, and of that fraction, 40-60% is used on space conditioning [1]. Despite a decrease over time in required energy per unit-area for space conditioning, there has not been a corresponding reduction in overall building energy consumption [1, 2], and for various reasons, building retrofits frequently proceed along sub-optimal paths both with regard to lifetime cost and energy use [3]. These factors combine to create an environment in which low-cost, low-labor products and behaviors with perceived energy-saving effects can thrive, sometimes without adequate scrutiny. There are many free or low-cost practices that do reduce energy use either outright (e.g. thermostat adjustment, weather-stripping, caulking [4]) or indirectly (e.g. fans [5–7]). But on the extreme end of the spectrum are products like "insulating paints" that promise effects comparable to or better than established best practices at lower cost and effort. Despite lacking appropriate peer review and relevant endorsements from standard-setting agencies, a slew of such products exist, and

nearly all present evidence meant to validate their performance claims. It is the goal of this paper to analyze potential energy savings from so-called insulating paints both theoretically and computationally in order to provide an independent benchmark of their potential effects. Computational fluid dynamics (CFD) has been used successfully to study thermal interactions within rooms under a wide variety of conditions and provides additional confidence in the conclusions made herein. For example, efforts to couple CFD with higher-level building simulation tools such as EnergyPlus [8] extend the abilities of both tools [9–12]. Further, CFD is often employed to directly analyze effects that would be lost in "well-mixed" analyses such as thermal-comfort impacts of forced-air supply locations [13], combined methods of space conditioning [14], and buoyancy-driven, non-energy-intensive space conditioning (displacement ventilation) [15, 16].

INSULATING PAINT – THEORY AND PREDICTIONS

Aside from aesthetics, paints and other surface coatings have a number of very utilitarian purposes. Specialty paints can provide protection against corrosion and abrasions and survive extremely harsh environments. With regard to energy savings, surface coatings are indisputably linked to radiative heat transfer. However, the class of products commonly known as insulating paints claim to provide thermal performance of magnitude comparable to labor-intensive building retrofits or efficient new construction at a fraction of the cost and effort. Given these extreme performance claims and the cost advantage that such products would have over traditional methods of insulation, it is worth rigorously examining what savings these products can actually achieve and why.

Advertising of residential insulation products in the U.S. is regulated by the Federal Trade Commission according to what is fa-
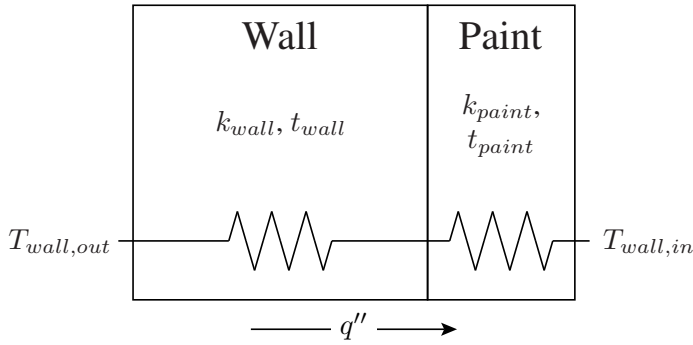
Figure 1: Thermal resistance circuit for a two-layer plane wall, where a plane thermal resistance is equal to t/k. t is thickness, k is thermal conductivity, T is temperature, and q'' is heat flux. Thickness of the paint layer is greatly exaggerated for clarity.

miliarly known as the "R-value rule." It sets out specific approved testing procedures that are required in order for a manufacturer or retailer to advertise the R-value of a product. Because the R-value is the most commonly understood measure of insulation performance, the regulation intends to protect consumers from misleading advertising. However, misleading claims abound. While some distributors of insulating paint refrain from claiming R-values altogether, others further confuse the issue by claiming that R-values are inapplicable to thin coatings. Even more, some rely on anecdotal evidence or seemingly official performance testing under inapplicable circumstances. In one such case, the manufacturer presents a variety of questionably controlled case studies and tests to justify claims of typical building energy savings of 20-40% [17], and these claims are specifically referenced to reduced conduction through the walls. A simple one-dimensional thermal resistance network for a wall and paint configuration is shown in Fig. 1. An elementary analysis reveals the steady heat flux in this scenario to be

$$q'' = \frac{T_{wall,out} - T_{wall,in}}{t_{wall}/k_{wall} + t_{paint}/k_{paint}} \quad (1)$$

where t_i and k_i are the thickness and thermal conductivity of the layer noted by the subscript, respectively, and $T_{wall,x}$ is the temperature of the wall at location x. It is apparent that heat flux scales inversely with the total thermal resistance of the wall, and that the magnitude of insulating paint's effect will be largest when the total resistance of the wall is low. Assuming fixed temperatures at the inner and outer surfaces of the wall, the addition of an insulating paint layer then results in a normalized reduction in heat flux equal to

$$1 - \frac{q_1''}{q_0''} = \frac{t_{paint}/k_{paint}}{t_{wall}/k_{wall} + t_{paint}/k_{paint}} \quad (2)$$

where q_1'' is exactly the heat flux depicted in Eqn. (1) and Fig. 1, and q_0'' is the heat flux in a control case with the same "wall" layer but without paint (i.e. $t_{paint} = 0$).

To apply Eqns. (1) and (2), various wall and paint properties can be assumed. The average thickness of a single (dry) paint layer can be assumed to be 50.8 μm based on a survey of paint manufacturers' (standard and insulating) product data sheets [18–21]. The total thickness of the paint layer is then based on how many layers are applied; the insulating paint manufacturer suggests three [21]. While standard acrylic paints have thermal conductivities of approximately 0.9 W m^{-1} K^{-1} [22], one particular manufacturer of insulating paint claims that a component of their product has the extremely low conductivity of 0.017 W m^{-1} K^{-1} [23]. Note that this unlikely value is roughly half the thermal conductivity of stationary air at standard conditions and on the order of published values for various aerogel products [24]. R-values of walls vary significantly with age of construction and quality of insulation. For example, while IECC guidelines for new construction in U.S. climate zone 5A recommend a wall R-value of 3.522 K m^2 W^{-1} (20 h ft^2 °F Btu^{-1}) and ceiling R-value of 6.692 K m^2 W^{-1} (38 h ft^2 °F Btu^{-1}) [25], a typical value for pre-1980 construction might be closer to 1.127 K m^2 W^{-1} (6.4 h ft^2 °F Btu^{-1}) [26]. From Eqn. (2), one expects insulating paints to see the most value in applications where wall R-values are low; thus to present their potential performance under favorable conditions, wall and ceiling R-values of 0.881 K m^2 W^{-1} (5 h ft^2 °F Btu^{-1}) were assumed for this work.

By application of Eqn. (2), a three-coat application of insulating paint with a "best case" (albeit unrealistic) thermal conductivity of 0.017 W m^{-1} K^{-1} applied to a 0.881 K m^2 W^{-1} (5 h ft^2 °F Btu^{-1}) wall would reduce q'' by only 1% at even these very generously assumed conductions. Higher inherent wall R-values will reduce energy savings accordingly to below 1%. For example, the aforementioned IECC recommended R-value of 3.522 W m^{-1} K^{-1} (20 h ft^2 °F Btu^{-1}) leads to a savings of only 0.25%. The 1D analysis can also be used to show that the low end of this manufacturer's predicted savings, 20%, would only be achieved with three coats of this extremely low thermal conductivity paint if the wall R-value were 0.036 K m^2 W^{-1} – roughly the R-value of only 0.61 cm of simple plaster board [27].

DESCRIPTION OF MODEL

To further examine how more complicated thermal interactions in a three-dimensional room might influence energy savings, CFD simulations were performed using ANSYS FLUENT v14.5 on a "cabin in the woods," an empty, square structure with four exterior walls. Details of input information are presented in Tables 1 and 2 while Fig. 2 shows an overhead view of the room. To save unnecessary computational expense, only one symmetric eighth of the room was modeled – this region is outlined.

As in Fig. 2, each wall's length was 3.048 m, the room's height was 2.4384 m, and the walls and ceiling were modeled as slab regions 0.25 m thick. A square air-supply inlet, 0.2 m on a side, was placed in the center of the room to mimic a forced-air heating/cooling system supply. Four air-exhaust outlets, each with a quarter of the area of the inlet, were placed 1.1 m from the center of the room on each major axis. These exhaust outlets can be
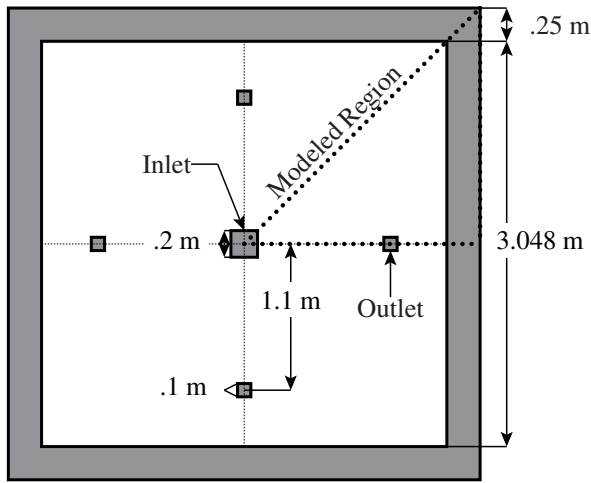
Figure 2: Overhead view of the room modeled in this work. The symmetric region used for CFD analysis is outlined with a dotted line. The interior height of the room was 2.4384 m, and the roof thickness was 0.25 m (not shown).
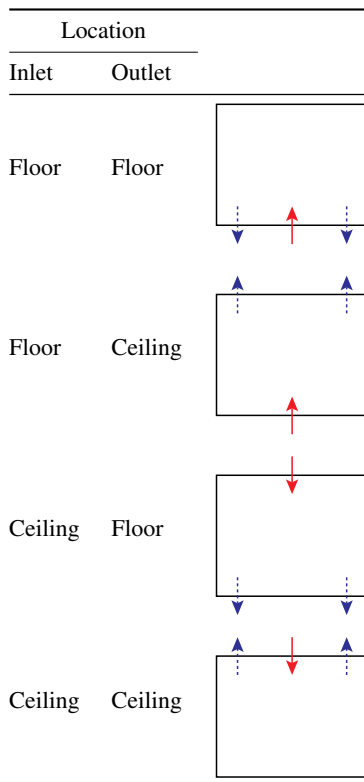

Figure 3: Side-view illustrations of the four room arrangements examined in this work. Solid red arrows indicate air inlets and dashed blue arrows indicate air outlets.

thought of as either the location of the return air registers and/or an aggregation of the leaks in the room through which air escapes to the outdoors, particularly when the heating/cooling system is running.

Missing from the fixed surface-temperature assumption of Eqn. (1) is the possibility for an insulating paint product to perform differently under heating or cooling scenarios due to secondary effects of temperature distribution, velocity patterns, etc. To account for this, separate computational analyses were performed for heating and cooling scenarios. As in Table 1, thermal boundary conditions were chosen to roughly represent the "Cold" (Building America) or 5A (IECC) climate zone [25], while conduction thermal transport properties were chosen to represent poor construction for that climate region, presumably creating a scenario in which simple, low-cost energy-saving measures have the most potential. In all cases, the floor was treated as perfectly insulated, all interior surfaces had emissivities of 0.9, and thermal conductivities of the 0.25 m thick walls and ceiling were defined to give an R-value of $0.881\,\mathrm{K\,m^2\,W^{-1}}$ ($5\,\mathrm{h\,ft^2\,{}^\circ F\,Btu^{-1}}$). As previously mentioned, this is far below the level of insulation currently required for residential construction in this climate region (walls–$3.522\,\mathrm{K\,m^2\,W^{-1}}$ [$20\,\mathrm{h\,ft^2\,{}^\circ F\,Btu^{-1}}$], ceiling–$6.692\,\mathrm{K\,m^2\,W^{-1}}$ [$38\,\mathrm{h\,ft^2\,{}^\circ F\,Btu^{-1}}$]) [25], and roughly comparable to the assumed values for pre-1980 midrise apartment buildings in reference models for the EnergyPlus building-simulation tool (the closest applicable building class) [26]. For heating (winter) cases, the exteriors of the roof and walls were specified identically: emissivities were 0.9 (gray, diffuse), convective heat transfer coefficients were $20\,\mathrm{W\,m^{-2}\,K^{-1}}$, and both the free-stream (convection) and surrounding (radiation) temperatures were $-8\,{}^\circ C$. For cooling (summer) cases, exterior walls were specified in the same way but with a free-stream/surrounding temperature of $28\,{}^\circ C$. The roof was specified with a fixed exterior temperature of $46\,{}^\circ C$ above ambient outdoor conditions to approximate the worst-case effects of solar load on a black surface [28] – in this case, $74\,{}^\circ C$. More detailed formulations of external radiative boundary conditions, such as effective sky temperatures and direct calculation of solar load, were not considered in this model since their impact on the behavior of the interior-facing, conduction-only insulating paint would be minimal, particularly in the context of relative energy savings.

In all cases, conditioned air was supplied to the room through a single inlet surface at prescribed temperature and velocity, and exited through an outlet surface that enforced conservation of mass for a steady, constant density flow. For heating cases, the inlet temperature was $43\,{}^\circ C$; for cooling, $11\,{}^\circ C$. Velocities were set to maintain the desired volumetric-average room temperature ($20\,{}^\circ C$ for heating cases, $22\,{}^\circ C$ for cooling). Selection of the inlet air temperatures was validated by comparing resultant steady-state airflow rates with industry guidelines for ductwork based on heating/cooling loads [29, 30]. These temperatures are summarized in Table 2. All simulation results are for steady-state conditions.

Because interior temperature stratification and airflow patterns

Case	Boundary	Mode	Parameter
Heating	Walls, Roof	Convection	$h = 20\,\mathrm{W\,m^{-2}\,K^{-1}}$
			$T_\infty = -8\,°\mathrm{C}$
		Radiation	$\varepsilon = 0.9$
			$T_{surr} = -8\,°\mathrm{C}$
Cooling	Walls	Convection	$h = 20\,\mathrm{W\,m^{-2}\,K^{-1}}$
			$T_\infty = 28\,°\mathrm{C}$
		Radiation	$\varepsilon = 0.9$
			$T_{surr} = 28\,°\mathrm{C}$
	Roof	Fixed T	$T_{roof} = 74\,°\mathrm{C}$
All	Walls, Roof	Conduction	$R = 0.8805\,\mathrm{K\,m^2\,W^{-1}}$
	Paint (per layer)	Conduction	$R = 2.988 \times 10^{-3}\,\mathrm{K\,m^2\,W^{-1}}$

Table 1: Exterior thermal boundary conditions and conduction transport properties for heating and cooling simulations. For convection, h is a heat-transfer coefficient and T_∞ is a free-stream temperature. For radiation, ε is emissivity and T_{surr} is the effective temperature of the surroundings. In cooling simulations, the exterior temperature of the roof is taken as a constant as discussed in the text. Conduction "R-values" are equal to t/k, where t is thickness and k is thermal conductivity.

Case		Temperature (°C)
Heating	Inlet	43
	Room Avg.	20
Cooling	Inlet	11
	Room Avg.	22

Table 2: Interior temperatures for heating and cooling simulations. The inlet temperature is specified for conditioned air entering the room. The "Room Avg." temperature is the desired volumetric-average temperature of the simulated room for that scenario.

vary significantly with placement of air supplies and exhaust [13, 15, 31], simulations were conducted for each of the four arrangements of inlet and outlets shown in Fig. 3 for both heating and cooling scenarios. The overhead view of the room (Fig. 2) remains the same in all cases. Therefore, a total of eight different scenarios were examined comprising heating and cooling for each of four supply/exhaust arrangements. While the 1D-analysis of Eqn. 2 suggested that insulating paints would have little impact on energy consumption in any case, it was important to model these different configurations to provide confidence in the results and subsequent conclusions. Additionally, since the effects of insulating paint are likely to be most significant in poorly designed or inefficient room arrangements, the outlets for all scenarios could be assumed as "leaks" directly leading to the outdoors. The room configuration's effect on temperature stratification will then directly impact the energy lost through those "leaks." Again, this enables examination of a system presumably most favorable to the use of insulating paints.

For each of the four geometries, a mesh of approximately 512 000 elements was constructed for one symmetric eighth of the room. The interior of the room was filled with tetrahedrons, with element size increasing with distance from interior surfaces. Solid regions subject only to steady heat-conduction were subdivided such that a relatively coarse, structured mesh could be created. Mesh density and element distributions were adjusted until good convergence was obtained as judged by FLUENT-reported residuals and overall heat transfer for the model (which for a steady-state model should be zero). Histograms of mesh "quality" for each room configuration (as computed by ANSYS ICEM CFD [32]) are shown in Fig. 4, where quality for a tetrahedron is simply its aspect ratio (0 to 1; unity is best). Mesh elements were of high quality overall. In all cases, 96%+ of elements had
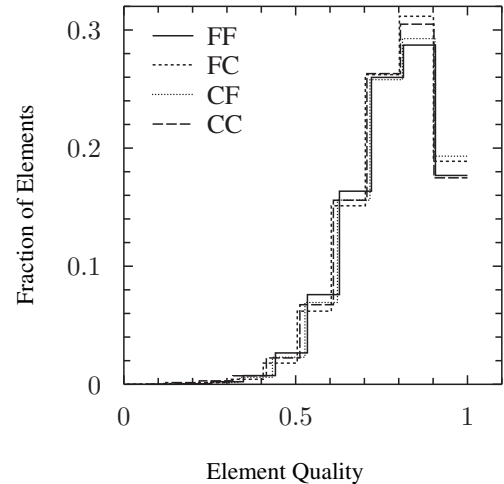

Figure 4: Histograms of element quality for each of the four room arrangements. The room configuration is indicated in the legend; for example, the inlet placed on the **F**loor and outlets on the **C**eiling is shown as **FC**.

quality ≥ 0.5, and approximately 75% had quality ≥ 0.7.

All simulations were conducted with constant-density dry air as the working fluid. Buoyancy effects were captured using the Boussinesq approximation with an expansion coefficient of $\beta = T_{room,avg}^{-1}$. Thermal conductivity and viscosity of the air were both temperature dependent using a piecewise interpolation of standard data and Sutherland's law, respectively. Turbulence was modeled with the standard $k - \varepsilon$ model as a good balance between computational expense and accuracy [33]. Interior radiation was solved under the assumption of gray, diffuse surfaces, and air was not considered to be a participating medium.

The effectiveness of insulating paint was examined by comparing heating/cooling power requirements of each room configuration with and without the presence of the insulating paint. In each scenario, an air inlet velocity was identified to maintain the room average temperature at the desired value (Table 2). This control case was then modified by the addition of 50.8 μm layers of insulating ($k = 0.017\,\mathrm{W\,m^{-1}\,K^{-1}}$) paint using FLUENT's "shell conduction" functionality for modeling thin walls in steady-state models. The equivalent "R-value" of an insulating paint layer is shown in Table 1. The inlet velocity was then iteratively adjusted to restore the desired room temperature. Simulations were conducted for both the insulating paint manufacturer's recommended thickness (three layers) and twice that thickness.

RESULTS AND DISCUSSION

Simulations were first conducted without the presence of insulating paint to establish control values for power consumption. As previously stated, inlet velocities were adjusted to achieve steady-state volumetric-average room temperatures according to Table 2. The power requirement for each scenario is reported in best- and worst-case metrics as follows. The least-possible space-conditioning power will occur in the case that there is no energy lost from the overall system by mass transfer, i.e. the inlet and outlets form a closed loop, and the only energy loss (or gain) occurs via conduction through the building envelope. For this extreme case, the power required for space conditioning is

$$\dot{Q}_{min} = \dot{m}\left(h_{in} - h_{out}\right) \qquad (3)$$

where $\dot{m}$ is mass flow rate, h_{in} is the (fixed) inlet enthalpy, and h_{out} is the outlet enthalpy. The worst-case metric assumes that *all* energy transfered by mass-flow through the outlets is lost, and the conditioning system must supply sufficient power to condition air from ambient outdoor conditions. In this extreme case,

$$\dot{Q}_{max} = \dot{m}\left(h_{in} - h_{amb}\right) \qquad (4)$$

where h_{amb} is the enthalpy of air at outdoor conditions as in Table 1. Control-case power consumptions by both metrics for all scenarios are reported in the $\dot{Q}$ row of Fig. 5. The $\dot{Q}_{min}$ metric is shown in the left column, and $\dot{Q}_{max}$ is shown on the right. The two-letter code on the top of each plot-column indicates the room configuration – e.g. **FC** refers to the configuration with the inlet on the **F**loor and outlet on the **C**eiling. Each configuration has an independent x-axis indicating the number of layers of insulating paint. Data for the "control" case is thus at $x = 0$. It is evident that the configuration of inlets and outlets within the room has a large effect on $\dot{Q}_{max}$ but little on $\dot{Q}_{min}$ – effects that are addressed in more detail by the authors in another article [34]. Interpreting the $\dot{Q}_{min}$ and $\dot{Q}_{max}$ metrics as requirements in tightly sealed and "leaky" structures, respectively, it is clear at a glance that the insulating paint is being evaluated over a wide range of operating conditions as intended.

After the addition of three or six layers of insulating paint to the model room, the inlet flow rate $\dot{m}$ was iteratively adjusted to restore the appropriate average temperature from Table 2 to a tolerance of 0.5 W in $\dot{Q}_{max}$. Resultant power consumption in each case is again plotted in the $\dot{Q}$ row of Fig. 5. Percent reduction in power consumption in both metrics for each case is shown in the bottom row of Fig. 5 computed as

$$100 \times \left(\dot{Q}_n - \dot{Q}_0\right)/\dot{Q}_0 \qquad (5)$$

where $\dot{Q}_n$ is power consumption with n layers of insulating paint, and $\dot{Q}_0$ is with zero. The 1D-analysis of Eqn. 2 predicted that a three-coat application of insulating paint would result in a savings of approximately 1% with the assumed R-values. Since the $\dot{Q}_{min}$ metric is equivalent to conduction-only losses, it is analogous to the 1D analysis, differing mainly in that it does not assume that wall temperatures remain fixed. The percent-reduction in $\dot{Q}_{min}$ for three layers of insulating paint is consistently $\approx 0.75\%$ across all test cases which is quite comparable to the results from the 1D analysis. The six-layer data-points show that the trend in power reduction is linear with the number of layers, as should be expected from Eqn. 2 given that the denominator is dominated by the wall/ceiling R-value and is thus effectively constant. In the worst-case metric, $\dot{Q}_{max}$, percent savings for three layers of insulating paint ranges from as little as 0.5% to 1% as a function of room configuration and whether the scenario is heating or cooling. This variation follows naturally from a further understanding of the $\dot{Q}_{max}$ metric. Expanding its definition

$$\dot{Q}_{max} = \underbrace{\dot{m}\left(h_{in} - h_{out}\right)}_{=\dot{Q}_{min}} + \dot{m}\left(h_{out} - h_{amb}\right) \qquad (6)$$

it is shown that $\dot{Q}_{max}$ differs from $\dot{Q}_{min}$ by the influence of the outlet enthalpy (since $\dot{m}$ is the same in both metrics, and h_{amb} is constant). Reduction or amplification of insulating paint's effects vs. the $\dot{Q}_{min}$ metric then must be due to changes in the room's temperature distribution (i.e. changes in the air temperature local to the outlets). In no case does the $\dot{Q}_{max}$ reduction exceed the prediction of the 1D analysis; in fact, most frequently it is below even the $\dot{Q}_{min}$ savings. The effects of insulating paint on h_{out} are thus minor, and most often, the significance of energy transport via mass flow limits the insulating paint's ability to affect overall energy consumption vs. the tightly-sealed case.

Convergence of these simulations was judged both by FLUENT-reported residuals and the model-wide net heat transfer rate, which for a steady-state simulation should be zero. Converged values of scaled residuals in x, y, and z-velocities as well as continuity were typically of order 10^{-7}, rising to 10^{-5} only in the **CC** geometry due to high velocities and strong buoyancy effects. Energy residuals were of order 10^{-7} or lower in all cases. Total model net heat transfer rates were on the order of 100 mW in the **CC** configuration, and 1 to 10 mW in others – many orders of magnitude lower than the space-conditioning power in all cases. Thus in each scenario examined, model convergence was excellent.

In short, both elementary thermodynamics and detailed 3D CFD simulations lead to the same conclusion about insulating
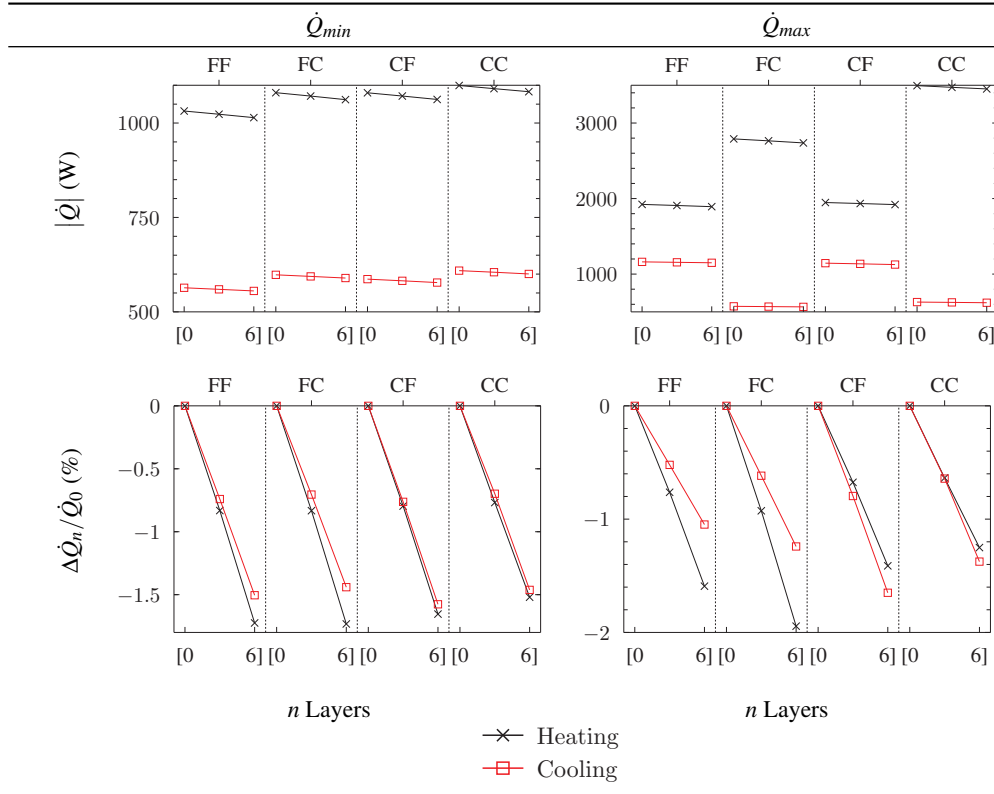
Figure 5: The effect of adding *n* layers of insulating paint on $\dot{Q}_{max}$ and $\dot{Q}_{min}$. The $\dot{Q}_{min}$ metric is shown in the left column and $\dot{Q}_{max}$ on the right. The top row shows raw values of the indicated $\dot{Q}$ metric, and the bottom row shows changes in that metric relative to the control case (*n* layers of insulating paint = 0). Within each plot, results from the four room geometries are shown on a common *y*-axis: the configuration is indicated at the top, and each has an independent *x*-axis (number of layers of insulating paint). A configuration labeled **FC** indicates inlet-**F**loor, outlet-**C**eiling.

paint: even with an extremely low thermal conductivity and a building with poor heat transfer properties that should have the most room for improvement, insulating paint cannot provide a significant barrier to conduction nor an opportunity for significant energy savings. The similarity in results between the theoretical investigation and CFD simulations under widely varied conditions provides confidence in the conclusions drawn herein.

CONCLUSION

Despite claims of extraordinary performance, the energy-saving potential of insulating paint was found to be minimal via an analysis of various "worst case" scenarios of application of this paint to a three-dimensional room. Both 1D and CFD analyses of conduction heat transfer through an R-5 wall suggest savings of 1% or less. In cases of high leakage of conditioned air to the outdoors, the savings is sometimes as low as 0.5%. Since a poorly insulated building will likely also be a poorly sealed building, this more pessimistic result suggests even further caution for performance expectations. Though this work relied on data from one particular insulating paint manufacturer when making assumptions about the properties of such products, the 1D analysis makes it apparent that these results apply to any thin coating claiming to be a conduction barrier. The ability of an insulating paint to pro-

vide energy savings lies in its ability to affect the total thermal resistance of a building's envelope. Even when the envelope's preexisting resistance is low and the paint is assumed to have an extremely low thermal conductivity, this analysis indicates that it is not reasonable to expect significant energy savings from current materials at the thickness of a few coats of paint.

REFERENCES

[1] Luis Pérez-Lombard, José Ortiz, and Christine Pout. A review on buildings energy consumption information. *Energy and Buildings*, 40(3):394–398, 2008. ISSN 0378-7788. doi: 10.1016/j.enbuild.2007.03.007.

[2] J. Laustsen. Energy efficiency requirements in building codes, energy efficiency policies for new buildings. *International Energy Agency and OECD*, 2008.

[3] Silvia Banfi, Mehdi Farsi, Massimo Filippini, and Martin Jakob. Willingness to pay for energy-saving measures in

residential buildings. *Energy Economics*, 30(2):503–516, 2008. ISSN 0140-9883. doi: 10.1016/j.eneco.2006.06.001.

[4] Gerald T. Gardner and Paul C. Stern. The Short List: The Most Effective Actions U.S. Households Can Take to Curb Climate Change. *Environment: Science and Policy for Sustainable Development*, 50(5):12–25, 2008. doi: 10.3200/ENVT.50.5.12-25.

[5] Fuad H. Mallick. Thermal comfort and building design in the tropical climates. *Energy and Buildings*, 23(3): 161–167, 1996. ISSN 0378-7788. doi: 10.1016/0378-7788(95)00940-X. PLEA '94 International Conference.

[6] Ruey-Lung Hwang, Ming-Jen Cheng, Tzu-Ping Lin, and Ming-Chin Ho. Thermal perceptions, general adaptation methods and occupant's idea about the trade-off between thermal comfort and energy saving in hothumid regions. *Building and Environment*, 44(6):1128–1134, 2009. ISSN 0360-1323. doi: 10.1016/j.buildenv.2008.08.001.

[7] Son H. Ho, Luis Rosario, and Muhammad M. Rahman. Thermal comfort enhancement by using a ceiling fan. *Applied Thermal Engineering*, 29(89):1648–1656, 2009. ISSN 1359-4311. doi: 10.1016/j.applthermaleng.2008.07.015.

[8] Drury B. Crawley, Linda K. Lawrie, Frederick C. Winkelmann, W.F. Buhl, Y.Joe Huang, Curtis O. Pedersen, Richard K. Strand, Richard J. Liesen, Daniel E. Fisher, Michael J. Witte, and Jason Glazer. Energyplus: creating a new-generation building energy simulation program. *Energy and Buildings*, 33(4):319–331, 2001. ISSN 0378-7788. doi: 10.1016/S0378-7788(00)00114-6.

[9] Zhiqiang Zhai, Qingyan Chen, Philip Haves, and Joseph H. Klems. On approaches to couple energy simulation and computational fluid dynamics programs. *Building and Environment*, 37(89):857–864, 2002. ISSN 0360-1323. doi: 10.1016/S0360-1323(02)00054-9.

[10] M. Mirsadeghi, B. Blocken, and J. Hensen. Application of externally-coupled BES-CFD in HAM engineering of the indoor environment. In *11th IBPSA Building Simulation Conference, Glasgow*, 2009.

[11] Zhiqiang John Zhai and Qingyan Yan Chen. Performance of coupled building energy and CFD simulations. *Energy and Buildings*, 37(4):333–344, 2005. ISSN 0378-7788. doi: 10.1016/j.enbuild.2004.07.001.

[12] Zhiqiang John Zhai and Qingyan Yan Chen. Sensitivity analysis and application guides for integrated building energy and CFD simulation. *Energy and Buildings*, 38(9):1060–1068, 2006. ISSN 0378-7788. doi: 10.1016/j.enbuild.2005.12.003.

[13] C.F. Gao and W.L. Lee. Optimized design of floor-based air-conditioners for residential use. *Building and Environment*, 44(10):2080–2088, 2009. ISSN 0360-1323. doi: 10.1016/j.buildenv.2009.02.011.

[14] Wei-Hwa Chiang, Chia-Ying Wang, and Jian-Sheng Huang. Evaluation of cooling ceiling and mechanical ventilation systems on thermal comfort using CFD study in an office for subtropical region. *Building and Environment*, 48(0):113–127, 2012. ISSN 0360-1323. doi: 10.1016/j.buildenv.2011.09.002.

[15] Zhang Lin, T. T. Chow, C. F. Tsang, L. S. Chan, and K. F. Fong. Effect of air supply temperature on the performance of displacement ventilation (part I) - thermal comfort. *Indoor and Built Environment*, 14(2):103–115, 2005. doi: 10.1177/1420326X05052563.

[16] Zhang Lin, T.T. Chow, C.F. Tsang, K.F. Fong, and L.S. Chan. CFD study on effect of the air supply location on the performance of the displacement ventilation system. *Building and Environment*, 40(8):1051–1067, 2005. ISSN 0360-1323. doi: 10.1016/j.buildenv.2004.09.003.

[17] Industrial Nanotech. Nansulate homeprotect home insulation coatings to insulate walls, attics, ceilings and more, 2014. URL `http://www.nansulate.com/homeprotect.htm`. Accessed: October 2014.

[18] Glidden Company. MSDS — Products — Glidden, 2014. URL `http://www.glidden.com/Products/MSDS`. Accessed: October 2014.

[19] Behr Process Corporation. Safety, Material Safety & Technical Data Sheets — BehrPro, 2014. URL `http://www.behrpro.com/BehrPro/prosafety/technical_library`. Accessed: October 2014.

[20] Sherwin-Williams Company. Data Sheets (PDS, MSDS, EDS), 2104. URL `http://www.sherwin-williams.com/painting-contractors/products/msds`. Accessed: October 2014.

[21] Industrial Nanotech. Nansulate homeprotect clear coat datasheet, 2014. URL `http://www.nansulate.com/pdf/Cutsheets/Nansulate_HPClearCoat_Cutsheet.pdf`. Accessed: October 2014.

[22] Ellen Brehob, Andre Desjarlais, and Jerald Atchlet. Effectiveness of cool roof coatings with ceramic particles. In *Proceedings of the 2011 International Roofing Symposium*, 2011.

[23] Industrial Nanotech. Nansulate liquid applied thermal insulation and mold resistance coatings, 2012. URL `http://www.nansulate.com/thermal_insulation_data.htm`. Accessed: June 2012.

[24] J Fricke and T Tillotson. Aerogels: production, characterization, and applications. *Thin Solid Films*, 297(12): 212–223, 1997. ISSN 0040-6090. doi: 10.1016/S0040-6090(96)09441-2.

[25] Pacific Northwest National Laboratory and Oak Ridge National Laboratory. High performance home technologies: Guide to determining climate regions by county (building america best practices series, volume 7.1). Technical report, U.S. Department of Energy, 2010. URL `http://apps1.eere.energy.gov/buildings/publications/pdfs/building_america/ba_climateguide_7_1.pdf`.

[26] National Renewable Energy Laboratory. U.S. Department of Energy Commercial Reference Building Models of the National Building Stock. Technical report, U.S. Department of Energy, 2011.

[27] Frank P. Incropera, David P. Dewitt, Theodore L. Bergman, and Adrienne S. Lavine. *Fundamentals of Heat and Mass Transfer, Sixth Edition*. John Wiley & Sons, 2007. Appendix A, Table A.11.

[28] Arthur H. Rosenfeld, Hashem Akbari, Sarah Bretz, Beth L. Fishman, Dan M. Kurn, David Sailor, and Haider Taha. Mitigation of urban heat islands: materials, utility programs, updates. *Energy and Buildings*, 22(3):255–265, 1995. ISSN 0378-7788. doi: 10.1016/0378-7788(95)00927-P.

[29] W. Johnson and K. Standiford. *Practical Heating Technology*. Delmar, Cengage Learning, Clifton Park, NY, USA, 2009. pg. 67.

[30] Carrier Air Conditioning Company. *Handbook of Air Conditioning System Design*. McGraw-Hill Book Company, New York, 1965. pg. 10-6.

[31] Qiong Li, Hiroshi Yoshino, Akashi Mochida, Bo Lei, Qinglin Meng, Lihua Zhao, and Yufat Lun. CFD study of the thermal environment in an air-conditioned train station building. *Building and Environment*, 44(7):1452–1465, 2009. ISSN 0360-1323. doi: 10.1016/j.buildenv.2008.08.010.

[32] ANSYS, Inc. Help manual—edit mesh—display mesh quality—quality. Documentation for ANSYS ICEM CFD 13.0, 2010.

[33] Q. Chen. Comparison of different k-ε models for indoor air flow computations. *Numerical Heat Transfer, Part B: Fundamentals*, 28(3):353–369, 1995. doi: 10.1080/10407799508928838.

[34] David J. Buckmaster and Alexis R. Abramson. The effects of interior emissivity and room layout on forced-air space conditioning power usage. 2014. Under review in *The International Journal of Heat and Mass Transfer*.